High pressure x-ray diffraction studies on nanocrystalline materials

2004 J. Phys.: Condens. Matter 16 S353

(http://iopscience.iop.org/0953-8984/16/5/003)

INSTITUTE OF PHYSICS PUBLISHING JOURNAL OF PHYSICS: CONDENSED MATTER

J. Phys.: Condens. Matter **16** (2004) S353–S377 PII: S0953-8984(04)70032-6

High pressure x-ray diffraction studies on nanocrystalline materials

B Palosz[1], S Stel'makh[1], E Grzanka[1,2], S Gierlotka[1], R Pielaszek[1], U Bismayer[3], S Werner[4] and W Palosz[5]

[1] High Pressure Research Centre UNIPRESS, ulica Sokolowska 29/37, 01 142 Warsaw, Poland
[2] Institute of Experimental Physics, Warsaw University, ulica Hoza 69, 00 681 Warsaw, Poland
[3] Mineral-Petrographisches Institut, Uni Hamburg, Grindelalle 48, D-20146 Hamburg, Germany
[4] Institut fuer Kristallographie, Uni Muenchen, Theresienstrasse 41, D-20146 Muenchen, Germany
[5] USRA/NASA-Marshall Space Flight Center, Huntsville, AL 35812, USA

Received 30 September 2003
Published 23 January 2004
Online at stacks.iop.org/JPhysCM/16/S353 (DOI: 10.1088/0953-8984/16/5/003)

Abstract

Application of the *in situ* high pressure powder diffraction technique for examination of specific structural properties of nanocrystals based on the experimental data of SiC nanocrystalline powders of 2–30 nm in diameter is presented. Limitations and capabilities of the experimental techniques themselves and methods of diffraction data elaboration applied to nanocrystals with very small dimensions (<30 nm) are discussed. It is shown that a unique value of the lattice parameter cannot be determined for such small crystals using a standard powder diffraction experiment. It is also shown that, due to the complex structure constituting a two-phase, core/surface shell system, no unique compressibility coefficient can satisfactorily describe the behaviour of nanocrystalline powders under pressure. We offer a tentative interpretation of the distribution of *macro*- and *micro*-strains in nanoparticles of different grain size.

1. Introduction

There is no unique definition of the 'nanocrystalline' state. A variety of definitions is given in the literature with a commonly accepted notion that the term 'nano' should be reserved for objects with physical dimensions not larger than 100 nm. We prefer definitions which do not refer to dimensions but to physical behaviour like that given by Navrotsky [1]: 'A nanomaterial is any state of condensed matter or of molecules by the emergence of a new phenomena not seen at smaller or larger scales' with an additional comment that: 'The exact size at which this happens depends both on the system and the property being considered'. This kind of definition can be verified experimentally and, indeed, common practice shows that the size dependence of specific physical properties occurs for dimensions below 100 nm. The fundamental basis for classification of material's behaviour is thermodynamics. In thermodynamic terms, at

first approximation, a nanocrystal behaves as a fragment of a larger size solid [2]. Based on that one could expect that nanocrystals exhibit properties similar to those of larger size objects of the same material. This concerns in particular phase transitions which should take place under the same p–T conditions. Experiments show, however, that in nanocrystals phase transition parameters are not rigorously defined, which conforms with the experimental findings that physical properties of very small crystals deviate significantly from those of the bulk. Referring to thermodynamics we can say that a material becomes 'nano' when its thermodynamic parameters differ significantly from those of the bulk due to diminution of its dimensions. It is certain that any change of a physical property of a material is accompanied by a change in its structure: the crystallographic structure (atomic arrangements or bond length, symmetry, polymorphism, etc), or microstructure (object dimensions, homogeneity, etc). The key problem is to understand what is the origin of differences in the properties between nano- and large-volume crystals, and how specific properties scale with the dimensions. We approach this problem through examination of the atomic structure of nanocrystals with application of diffraction methods.

Experimental evidence suggests that crystallographic structure of a very small size particle is perturbed relative to that in the bulk crystals, which is reflected in changes of the phase transition conditions (temperature and/or pressure). For instance, in metal powders it is observed that the melting temperature decreases significantly with a decrease in the grain size [3]. It was implied that the surface of nanocrystals acts as a perturbation of the total free energy of the grains. In solid–solid transitions in nanocrystals the differences in surface energy between the two structures produce a shift in the phase transition pressure as a function of the nanocrystal size. For example, a shift to lower transition pressure with increasing size observed in CdSe nanocrystals is explained by higher surface energy in the high pressure rocksalt relative to the wurtzite structure [2].

It is obvious that the surface energy depends on the external crystal faces and that the structure at the surface is generally different from that in the bulk. The rearrangement of atoms at the surface may involve a preferred exposure of specific atoms or components at the external layer. The question of specific surface properties needs to be resolved separately for solid–gas, solid–solid and solid–liquid interfaces. For non-isolated, agglomerated nanoparticles and for dense nanocompacts the term 'interface' is more appropriate than 'surface': it has been suggested that interfacial enthalpies are one order of magnitude smaller than the surface enthalpies [4].

When considering the influence of the surface on the phase stability of nanocrystals one expects the surface entropy to be higher than that in the bulk (the atoms are less tightly bound at the surface which leads to higher vibrational entropy). Thus the surface free energy G_{surface} is usually lower than the surface enthalpy H_{surface}. Typical surface enthalpies are on the order of 0.1–3 J m^{-2}. That means that for nanopowders with a surface area of 200 m^2 g^{-1} the enthalpy increases by 2–60 kJ mol^{-1}. For a number of polymorphic materials with similar free energies this difference is large enough to affect phase transitions [1]. This work is dedicated to examination of the elastic properties of SiC nanocrystals not exhibiting phase transitions within the examined pressure range. The effect of the surface of nanocrystals on their behaviour under pressure, which is the subject of this article, concerns generation and distribution of *macro*- and *micro*-strains and their dependence on the grain size in nanocrystalline powders of SiC. The basic experimental technique used for this work is compression of nanopowders without a pressure medium (the so called isostatic pressure conditions). Such a technique gives us a unique opportunity to exaggerate the effects of generation of strains originating at the contacts between the individual grains (dependent on the specific structure of the grain surface) on the material properties.

2. Model of a nanocrystal

A unique model of the atomic structure of very small crystals to which the measured specific properties could be referred does not exist. A model of a nanocrystal where a structurally uniform grain core is surrounded by a surface shell with a different structure (which can also be interpreted as a two-phase system [5]) has been discussed in the literature but the concept has never been verified experimentally. Recently we examined theoretically a core–shell model of nanocrystals where the core is a well defined crystallographic phase while the surface shell has atomic structure different but similar and correlated to that of the grain core [6–8]. When building the model of the surface structure one has to account for the driving force making the atoms depart from their perfect lattice positions. In general, to decrease the energy of the actual crystal surface, a given structure can undergo relaxation or reconstruction. The materials with non-directional bonds (like metals) tend to undergo relaxation, while those with directional bonds (like Si) 'choose' reconstruction. The driving force for relaxation of metal surfaces is that the first surface layer is in a medium with a lower average electron density than its bulk counterparts which leads to reduced oscillatory relaxation when moving from the surface to the bulk. On the other hand, the broken directional bonds at the surface (e.g. Si) bring the surface atoms to a strongly unstable state. In response, the atoms undergo strong elastic distortions and rearrange themselves to form a new structure with fewer dangling bonds [1, 2].

When building a model of nanocrystalline SiC we assumed the presence of a surface strain at the surface. This strain leads either to elongation or shortening of the Si–C, C–C and Si–Si bonds relative to the relaxed SiC lattice. We verified this model experimentally, showing that diffraction data obtained for a very large diffraction vector range is sensitive enough to detect even small differences between interatomic distances in the grain's core and shell [6–8]. According to the core–shell model (which is essentially a two-phase model) the properties of nanocrystals should be referred to the two phases of the material and not to a single, uniform structure characteristic for bulk crystals. This should apply to any physical property of a nanomaterial. In this paper we discuss derivation of the elastic properties of nanocrystals for SiC nanopowders examined with *in situ* high pressure diffraction techniques.

3. Application of powder diffraction to examination of nanocrystals

The analysis of powder diffraction data is routinely performed using the concept of the unit cell and the Bragg equation [9, 10]. An alternative method of elaboration of powder diffraction data, developed for materials showing a short range order (like liquids and glasses), is the PDF (known also as rdf—radial distribution function) analysis leading to determination of the atomic pair distribution function, $G(r)$ [11–14]. Both methods are illustrated in figure 1. The structural parameters which can be derived from powder diffraction data are presented schematically in figure 2. In a standard powder diffraction experiment one uses only characteristic scattering, the Bragg reflections. The lattice parameters can be calculated from the reflection positions while information on the material microstructure (in particular the *micro*-strains generated under pressure) can be deduced from the reflection profiles. One has to remember that a diffraction experiment provides information on the structure of the material averaged over the whole sample volume illuminated by the beam. For that reason any quantitative information derived from a diffraction experiment provides average values only: the positions of the Bragg reflections are determined by the 'average lattice parameter' (which averages atomic vibrations, strains, and other crystal imperfections); PDF analysis provides information on specific interatomic distances averaged over all corresponding atomic pairs in the sample.

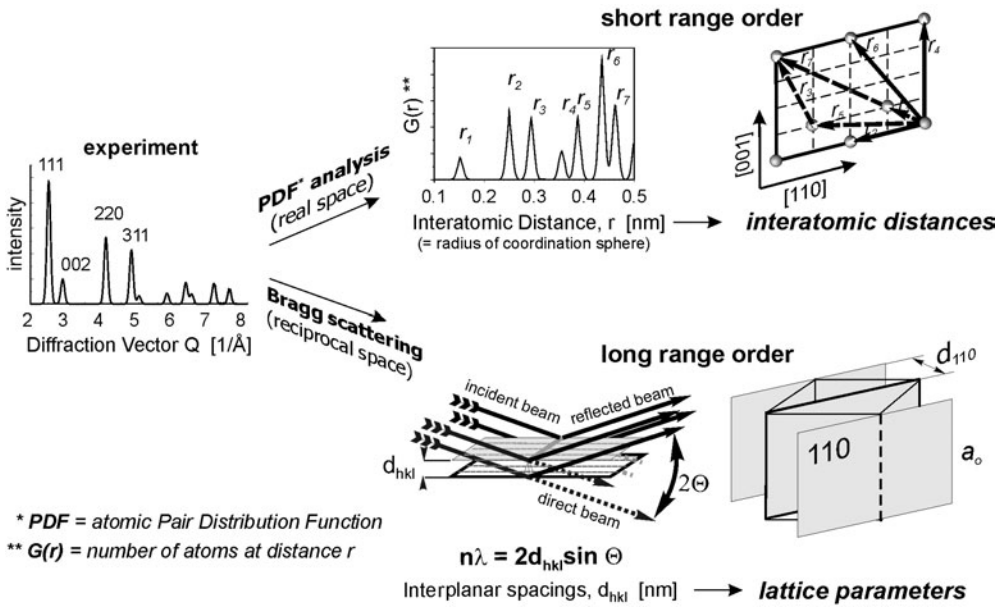

Figure 1. Two methods of elaboration (and interpretation) of a powder diffraction experiment.

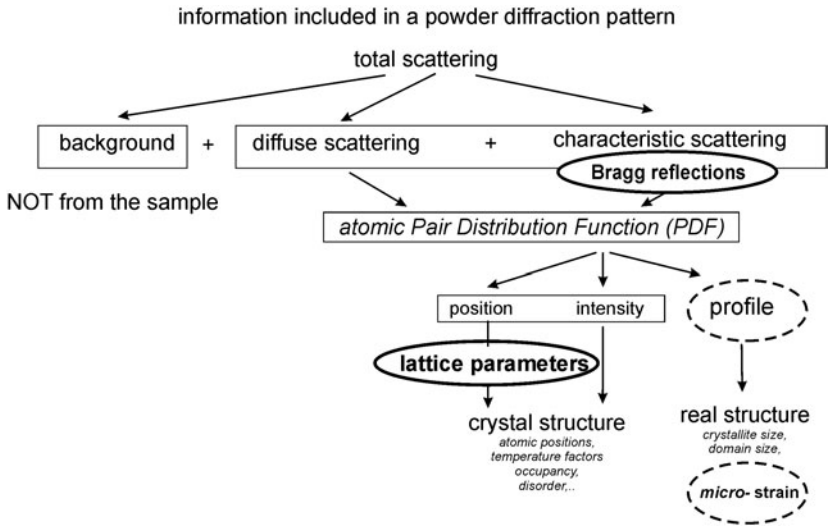

Figure 2. Structural parameters which can be derived from powder diffraction data.

3.1. Analysis of long-range atomic order in nanocrystals: application of the Bragg equation

Nanocrystals, although very small, are, by definition, single crystals. As such, they belong to the class of materials with a long-range atomic order and thus, in principle, appropriate methods of elaboration of the diffraction data can be based on the Bragg-type scattering. For a perfect, infinite crystal the positions of all individual Bragg reflections are determined uniquely by the Bragg equation, thus the lattice parameters can be calculated from any set of individual reflections (for cubic structures it can be calculated even from a single reflection:

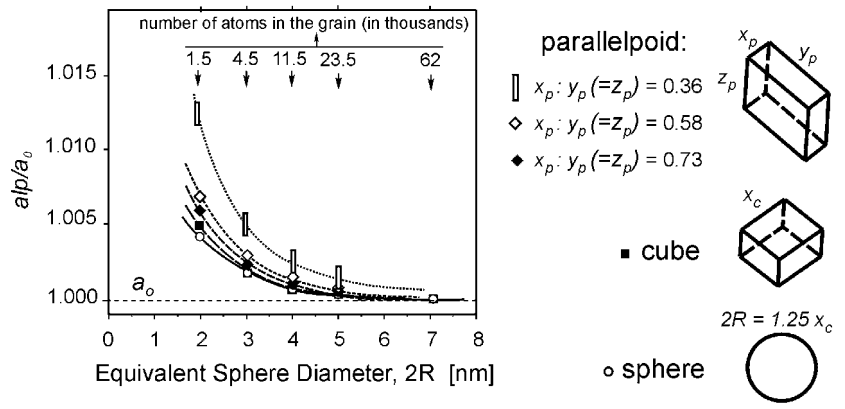

Figure 3. Dependence of the alp/a_0 ratio on the grain size calculated from the (111) Bragg reflection of a diamond nanocrystal for different crystallite shapes.

$1/d_{hkl} = (h^2 + k^2 + l^2)/a_0^2$). However, in nanosize grains, the long-range order is limited by the size of the crystallite, that can be smaller than the coherence length of the scattered beam. In this case the Bragg equation may not be applicable since the positions of the Bragg reflections are not determined by the unit cell parameters alone but become strongly influenced by the grain size and shape [6–8]. This effect is demonstrated in figure 3 showing the lattice parameters (in terms of the ratio alp/a_0) of the cubic unit cell of diamond calculated from a single (111) reflection of theoretical diffraction patterns which have been computed for models of a diamond nanocrystal with a perfect crystal lattice but different shape and size. (*Note that in figure* 3 *we use the term 'alp' (apparent lattice parameter, cf next section) instead of the lattice parameter* a_0 *since the latter, used to build the model, is not equal to the values calculated from the (111) reflection.*)

3.2. The meaning of the lattice parameter in a perfect crystal lattice of very small crystals

A number of papers has been published on a dependence of the lattice parameters on the grain size for a variety of nanomaterials, like metals (Co [15], Fe [16], Au [17, 18], Al [19], Cu [20]), semiconductors (CdSe [21], GaN [22]), ionic crystals (NaCl, KCl, NaBr, LiF [23], Y_2O_3 [24]), and others (e.g. Se [25]). Those results are often attributed to the presence of an 'internal pressure' caused by the surface stresses analogous to the surface tension in liquids [26–35]. Accepting that the 'lattice parameter' reflects the strength of the atomic bonds, it is natural to relate and describe various physical properties to the 'lattice parameter' which should correlate with specific materials behaviour. As we showed in the preceding section (figure 3), for very small crystals (several nanometres in dimensions) this parameter (determined from a standard powder diffraction experiment) loses its unique meaning and, therefore, has to be interpreted with caution.

Recently, we proposed a methodology of analysis of powder diffraction data of nanocrystals based on calculations of the lattice parameter values from individual (or a group of) Bragg reflections [6–8]. We call such calculated quantities, which are linked to the Q-values of the corresponding reflections, the 'apparent lattice parameters', alps. Diffraction patterns of simple structures have well separated individual reflections, thus their alp values can be calculated for each individual peak (figure 3). (*Note: the dependence of alp values on* Q*-vector is a discrete relation. However, to emphasize the general trend, we connected respective*

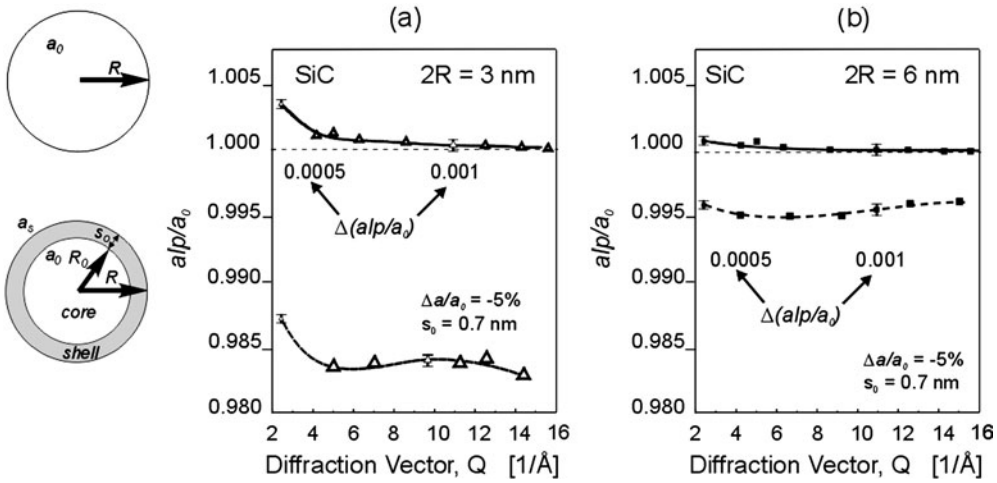

Figure 4. Dependence of the alp/a_0 ratio on the diffraction vector Q for spherical grains of SiC with (a) one uniform phase and (b) a core–shell structure.

individual alp values with arbitrary curves.) No simple analytical function describing a dependence of alp values on the Q-vector exists. Therefore, we evaluate the crystal structure based on a comparison of the experimental and theoretical alp–Q relations.

As follows from the above, for very small crystals with a perfect atomic structure, determination of the unique (true) values of the lattice parameters based on diffraction data is very laborious (if not just impossible): it requires measurements of the Bragg scattering up to a very large Q-value and, then, matching the experimental alp–Q dependence with those calculated theoretically for different models of the nanocrystal. The problem becomes even more complex when the structure of a nanocrystal is composed of the grain core and the surface shell (each having a different atomic structure). In a diffraction experiment it is practically impossible to separate the signals from the grain core and those from the surface shell: the beam scattered by the core atoms interferes with that scattered by the surface atoms. It is obvious that a single set of 'lattice parameters', which is unique only for a single crystal phase, is inappropriate for a description of such a complex structure. To evaluate the atomic structure of a nanocrystal with a core–shell structure, the alp concept appears particularly useful. Our model of a spherically shaped nanocrystal (see the diagram in figure 4) has a grain core of radius R_0 with a uniform crystallographic structure unambiguously characterized by the lattice parameter a_0. We assumed that the atomic structure of the surface layer (of width s_0) is correlated with the parent structure of the grain such that it is basically the structure of the core but centro-symmetrically deformed. To describe the model we introduce the parameter a_s which corresponds to the lattice parameter a at the outmost atomic layer of the particle. Assuming that the arrangement of atoms in the surface shell is similar to that in the grain core, the value of a_s is a fraction of the lattice parameter a_0. Without compression the width of the surface layer would be s_0. The actual values of the inter-atomic distances within the surface shell are expressed as a function of the distance r from the particle centre and vary between a_0 in the grain core (at distances $r \leqslant R_0$) and $a_s = a_0 + \Delta a$ (for $r = R_0$). The ratio $\Delta a/a_0$ quantifies the surface strain.

The effect of the presence of the surface shell on the alp values determined from a powder diffraction experiment calculated for spherical grains is shown in figure 4. The figure presents theoretical alp/a_0–Q-plots determined from diffraction patterns of simple models of

nanocrystals of SiC with (i) a perfect crystal lattice and (ii) a core–shell structure with a uniform compression of the surface shell lattice. These alp–Q-plots were calculated for crystallites of 3 and 6 nm in diameter with the surface shell 0.7 nm in thickness and all inter-atomic distances within the shell compressed uniformly to $\Delta a/a_0 = -5\%$.

Note. In the presence of surface strains the individual Bragg lines become slightly asymmetric. The reflections of very small nanocrystals with a relaxed lattice are very broad (for a 3 nm crystallite they are 0.22 and 0.25 Å^{-1} in width, for a 6 nm grain they are 0.12 and 0.13 Å^{-1}, at $Q = 2.5$ and 10 Å^{-1}, respectively) and asymmetry associated with the surface strain has a very small effect on the calculated peak positions. To fit the line shapes we used the PeakFit 4.0 for Windows program from SPSS Science. We assumed that the difference between peak positions calculated for individual peaks using symmetric pseudo-Voight and split Pearson shape functions is a measure of uncertainty (error bars in figure 4) of the calculated positions of the Bragg lines. The results shown in figure 4 were calculated by refinement of the alp values for selected Q-ranges (not for individual reflections). The errors of such calculated alp/a_0-values are not larger than those calculated for individual reflections.

Figure 4 shows that, for a model with compressed surface layer, the calculated alp values are lower than those of the relaxed lattice in the whole Q-range. The decrease of alp values is larger for smaller grains because, for a given thickness of the shell, the relative number of core to shell atoms strongly increases with an increase in the crystallite diameter. There is a distinct difference between alp–Q-plots of the one-phase and core–shell models. For a one-phase structure the largest alp value occurs for the smallest Q and decreases gradually approaching the real value at very large Q. For the structure with a strained surface shell the alp/a_0–Q-relation shows a complex dependence with some characteristic minima and maxima. This feature is obviously related to the presence of a two-phase system and can be used for identification and evaluation of the surface structure [6–8]. (*Note that the presence of homogenous strain in the sample volume, corresponding to the simple concept of internal pressure, would lead to a change of all alp values to the same degree without changing the shape of the dependence of alp on Q.*)

4. High pressure studies

In situ high pressure (hp) powder diffraction experiments are widely used to examine the strength of interatomic interactions through determination of the material's compressibility [36, 37]. As shown in figure 5, the interatomic potential of a two-atom system, ϕ, depends on the distance between the atoms and has a minimum determining the equilibrium interatomic distance r_0. Application of an external force along the interatomic bond leads to a change of the distance r according to the relation $F = \delta\phi/\delta r$ (figure 5(a)). The effect of stress is determined by measurements of the overall properties of the bulk material. This can be done experimentally by application of a homogenous stress (hydrostatic pressure) which can be accomplished using a fluid medium.

Behaviour of solids under pressure is conventionally characterized by the bulk modulus B_0 defined as the relative change of the volume of the sample per unit change of the applied external (hydrostatic) pressure. In the elastic region of the compression curve the relative change of the volume, $\delta V/V$, is proportional to the change of the applied pressure δP, equation (1):

$$B_0 = -V(\delta P/\delta V)_T. \tag{1}$$

Beyond the elastic region, a further increase in pressure leads to a decreasing compression of the material (figure 5(b)). Several equations of state describing this nonlinear behaviour were

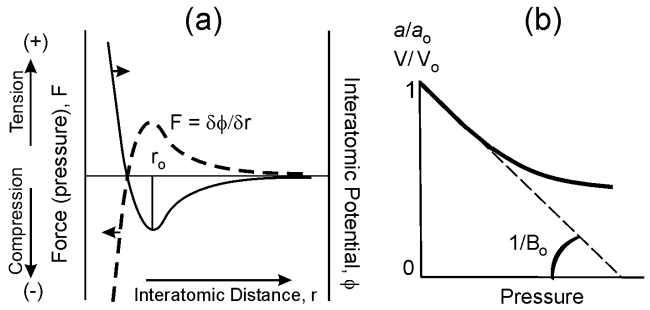

Figure 5. Compression in materials: (a) interatomic potential and related interatomic force; (b) compression curve.

proposed [36, 37]. In this work we examine the structural changes in nanocrystalline powders based on the analysis of the experimentally determined changes of the lattice parameters. The analysis concerns compression of the entire crystal lattice (formation of *macro*-strains) and generation of *micro*-strains in the structure. (*Note: we do not discuss phase transitions in the materials and, thus, we do not examine relations between crystallite dimensions and thermodynamic stability conditions.*)

Elastic properties of crystalline materials are described based on the bulk modulus which applies to any form and shape of a crystalline material: single crystals, polycrystals, crystalline layers, etc. From this point of view, no particular techniques of high pressure studies, nor any special methods of diffraction data elaboration, are required in the investigation of nanocrystalline materials. However, as will be shown in this work, interpretation of the experimental diffraction data of nanocrystals collected under external stresses (high pressure) is very laborious and requires application of some non-standard experimental and theoretical methodologies. This is due to (i) the presence of internal strains (pressure) in as-grown nanograins [38–41] and (ii) non-uniform atomic structure of nanocrystals resembling rather a two-phase than a one-phase material [5]. In addition, a description of the atomic structure of nanocrystals by the lattice parameters is questionable: the values of the lattice parameters determined from the Bragg equation are not unique (cf sections 3.1 and 3.2).

In this work we will discuss specific problems with conducting and elaborating the results of high pressure diffraction experiments on nanocrystals:

(i) compression of nanocrystalline powders without a pressure medium, i.e. under the so-called isostatic pressure conditions (we call this process 'densification') and
(ii) compression of nanopowders under hydrostatic pressure conditions [42–47].

As we will show, interpretation of the differences between elastic and non-elastic properties of bulk and nano-scale crystals is not straightforward since nanocrystals can be considered either as a single or a complex, multiphase structure. Our discussion of the effects of application of external stresses to nanopowders, and interpretation of our hp diffraction experiments on nanocrystalline SiC powders, will be based on a core–shell model of nanocrystals.

4.1. Experimental aspects of powder diffraction under high pressure

High pressure diffraction experiments require special equipment and procedures [36, 37, 48–50]. Application of high pressure to a sample requires special constructions where a certain amount of the sample is tightly closed in a volume to which an external stress

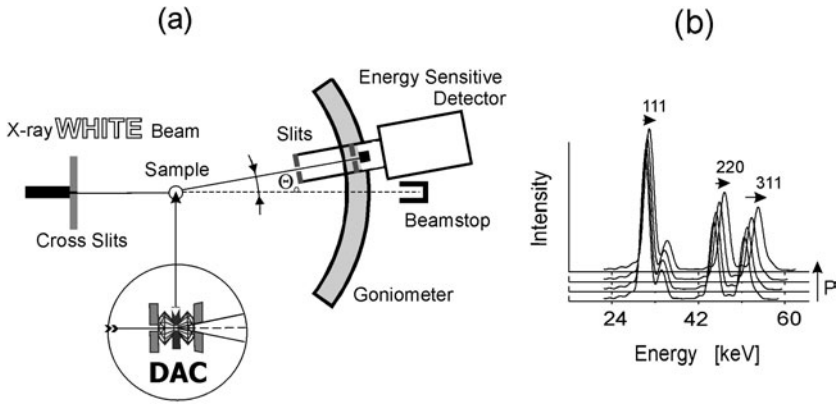

Figure 6. Powder diffraction under high pressure in the energy dispersive geometry. (a) Configuration of *in situ* experiments; (b) evolution of the powder diffraction pattern of SiC with an increase in pressure.

is applied. Due to technical limitations of the materials exposed to extreme loads, the volume in which the pressure can be generated strongly decreases with an increase in the maximum pressure available in the apparatus. Equipment capable of withstanding a pressure of tens of gigapascals can accommodate samples up to about 0.001 mm^3 in size. The commonly used sample holder is the diamond anvil cell (DAC).

In the most common configuration of a powder diffraction experiment the diffracted intensity is measured by a detector which scans over the diffraction angle of 2Θ. Because the diamonds which generate pressure have to be supported by a strong, massive construction, the access to the sample area is limited to a relatively small angle about the DAC axis. For that reason the most suitable technique for those measurements is the energy dispersive geometry, where the diffraction pattern is collected as a function of the energy of the beam diffracted at the (fixed) detector angle Θ_0 [37], as shown in figure 6. For such geometry the Bragg equation written as a function of energy is

$$2d_{hkl} \sin \Theta_0 = \lambda_{hkl} = hc/E_{hkl} = 12.398/E_{hkl}, \tag{2}$$

where h is the Planck's constant, c the velocity of light, d_{hkl} the interplanar spacing, and E_{hkl} the energy of photons (in kiloelectronvolts) obeying the Bragg equation for a given d_{hkl}. The experimentally accessible range of the measured d_{hkl}-values depends on the detector angle Θ_0 (figure 7). This condition is similar to selection of the wavelength of the incident beam in the angular dispersive geometry of diffraction experiments.

For polycrystalline materials it is convenient to determine the pressure inside the sample volume using internal pressure markers. The marker is a relatively soft material (small bulk modulus) with a known compressibility. A very small amount of the marker is mixed with the sample and the signals from the sample and from the marker are registered simultaneously during the experiment. The pressure in the cell can be calculated from the measured positions of the Bragg reflections of the marker (figure 7).

Most hp diffraction experiments are performed under hydrostatic pressure conditions. Such measurements can be made using solid or liquid pressure media like NaCl, vaseline, oils, alcohols, liquid argon, etc [36]. Hydrostatic conditions are very difficult to accomplish in very small volumes such as that in DAC where surface effects play an important role in generation of strains in the compressed sample material. This creates a particularly severe problem with brittle (non-plastic) polycrystalline materials where individual powder grains

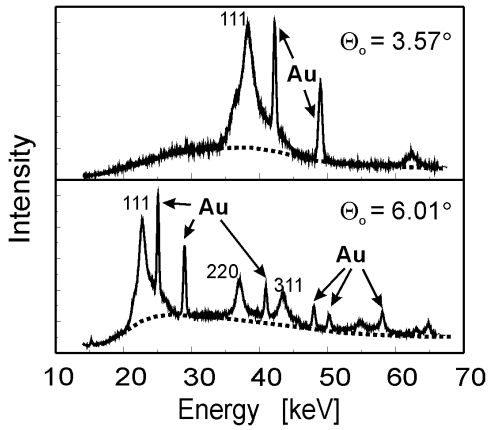

Figure 7. Diffraction patterns of 4 nm powder of cubic SiC measured in a DAC at different detector angles Θ_0; Au is the pressure marker.

are in direct contact. Therefore, a very careful interpretation of the powder diffraction data collected with DAC is necessary, particularly at lower pressures when the contact area between the grains is very small, which can lead to extreme stresses at the contact points.

We performed our diffraction measurements in Hasylab at DESY using a diamond anvil cell (DAC-station F3) capable of exerting pressures up to 45 GPa at room temperature. Using the energy dispersive geometry, diffraction patterns with the diffraction vector values up to 3.5–4 Å^{-1} and with a reasonably good statistics were taken. For higher Q-values good quality data could not be obtained due to a poor signal-to-background ratio. To obtain diffraction data for larger Q-values, measurements in a DAC in the angular dispersive geometry using laboratory Mo Kα_1 radiation were also made (cf section 5.3).

Note: The experimental set-up and the capabilities and limitations of the F3 station at Hasylab which we used for our measurements have been discussed in detail by Otto [49]. One of the critical problems in evaluating EDX diffraction data is accounting for resolution of the instrument which is a function of energy, and depends on the diffraction angle and the detector characteristics. This is particularly important for quantitative evaluation of the diffraction data measured in a wide energy range and used for structural refinement (usually using the Rietveld methodology) [37, 50]. For nanocrystalline samples examined in this work we analysed a change of the position and broadening of (111) SiC reflection measured around 30–40 keV. The experimental resolution for this energy range is $\Delta E/E \approx 0.2$–0.3 keV [49]. The change of resolution with energy is negligible relative to the uncertainty of determination of the peak positions and has been ignored. The full width at half maximum (FWHM) of nanocrystalline SiC is much larger than the resolution and varies between 0.5 and 2.5 keV for 30 and 2 nm grain size, respectively (figure 14). In our study we focused on a comparative study of various kinds of nanocrystalline SiC; we did not attempt to determine the absolute values of the lattice parameters but to measure relative changes of the position and broadening of individual Bragg reflections. Due to a very large broadening of the peaks the only practical method to get reproducible results is to select a common shape function for elaboration of all data used in the study. The accuracy of determination of the peak parameters is very strongly dependent on the correction for the background intensity. The error bars shown in figures 13, 14, 16 and 17. were evaluated by fitting the line shapes (applying the PeakFit program) using different background intensities and selecting different energy ranges about the peaks. Standard deviations derived

directly by the fit program for FWHM of a single peak are very small. We assumed that the width of the measured intensity maxima is equal to about half of the width of a single detector channel, 0.27 eV [49].

We performed a series of hp diffraction experiments on nanocrystals in DAC using different pressure media and found that the results were dependent on the medium used: liquid Ar, mixture of alcohols, vaseline, or silicon oil. The results obtained under hydrostatic pressure presented in this work were done using silicon oil as the pressure medium. Other experiments discussed in this work were done without a pressure medium, i.e. under so-called isostatic pressure conditions [43–47]. The measurements resemble the actual conditions of densification and sintering techniques, so such an experimental configuration provides an insight into real and important technological processes.

4.2. Elaboration of powder diffraction data measured in situ under pressure

A number of papers were published on examination of polycrystals under pressure using diffraction methods. They concern compressibility, deviatoric stresses, *micro*-strains, yield strength, etc [36, 37, 51–53]. In this work, dedicated to nanocrystalline SiC powders, we will attempt to find out if there are any specific properties of this material which are dependent on, and correlated with, (1) the grain dimensions and (2) the surface of the crystallites. For 'ordinary polycrystals' both such effects can be ignored, but they may be significant in nanopowders. In the analysis of the lattice compression we also have to keep in mind that the lattice parameters determined from the positions of Bragg reflections are, in fact, the 'alps'. Therefore, due to uncertainty as to the real meaning of the measured values of the lattice parameters, we will not make any quantitative evaluation of the elastic properties of SiC nanocrystals. To make a quantitative data evaluation one has to determine whether a nanocrystalline species constitutes a one- or two-phase (core–shell) grain. In this work we attempt to determine the type of the real structure of nanocrystals. Only then will we be able to discuss other issues, e.g. should nanocrystalline powder be characterized by one (bulk) or two moduli (that of the core and that of the shell). A similar dilemma concerns the yield strength of nanocrystals.

In the diffraction experiments on powders under pressure, which are the subject of the present study, we intended to investigate *macro*- and *micro*-strains generated in the materials. Both types of strain have to be regarded as sample parameters, as illustrated in figure 8. The relative change of the lattice parameters per unit pressure interval provides the measure of *macro*-strains, $(\Delta a/a)/\Delta P$. *Micro*-strains lead to a variation of the lattice parameters about the average value. As shown schematically in figure 8, the presence of *macro*-strains in a crystalline material is reflected in the diffraction pattern in the shift of the Bragg reflections from their reference positions (without changing the peak width, figure 8). The presence of *micro*-strains leads to broadening of the Bragg reflections. When *micro*-strains cause a change in the average lattice parameter of the sample, the broadening is accompanied by a shift of the peak position as well (figure 8). To determine the positions and widths of the Bragg reflections we used, as the standard procedure, a fit of the shape of the experimental peaks to the pseudo-Voight or split-Pearson functions [10, 54]. The split-Pearson function allows for an independent fit of the left and right shoulders of the peaks and can be conveniently applied for both symmetrical and asymmetrical shapes. This way we are able to get rid of the strong scatter of the measured intensities (which is very critical in high pressure experiments due to very low net intensities of the peaks) and obtain reproducibly the intensity profiles of all reflections. The positions of the reflections were taken at the weighted centre of intensity of the refined (fitted with the split-Pearson function) reflections.

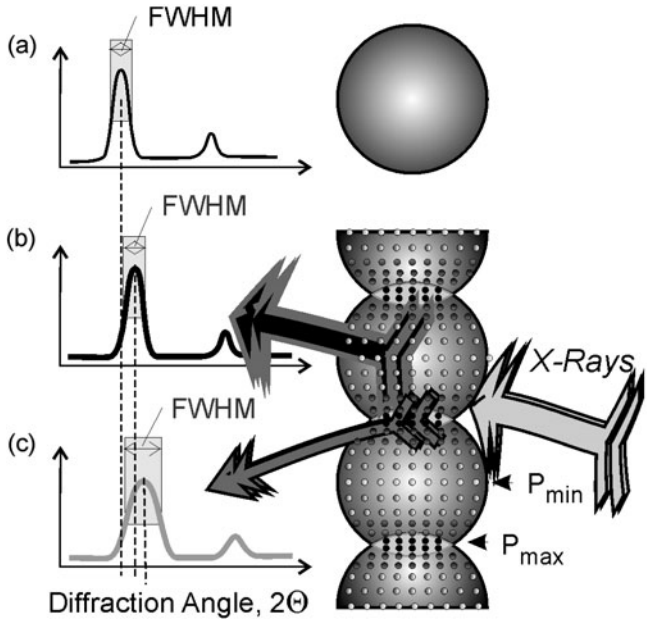

Figure 8. Effect of the presence of *macro*- and *micro*-strains on the position and width of the Bragg reflections. (a) Relaxed lattice; (b) *macro*-strains; (c) *micro*-strains.

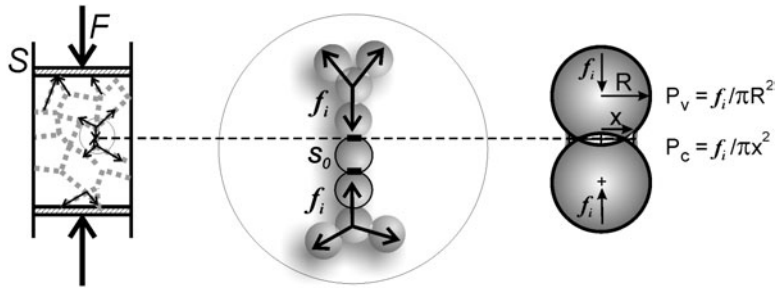

Figure 9. Model of distribution of microstrains during densification of a powder sample.

5. Sources of non-uniform distribution of strains in polycrystals under external stresses

For high pressure diffraction experiments it is a common practice to determine the pressure based on the Bragg reflections of the internal standard (here Au). Strictly speaking, the term 'pressure' is fully appropriate only if the applied external stress (load) is transferred to the material through a hydrostatic medium. A ceramic powder placed in a DAC without a pressure medium is a porous material, thus the term 'pressure applied to the sample' is not fully adequate. The external load applied to the diamond anvils is transferred to the sample through the grains which are in direct contact with the anvils (figure 9). The stresses are transferred to the grains underneath and, through the contact points between the grains, the external load is evenly distributed across the entire sample volume. The local pressure is the actual stress transferred by the material (a chain of grains) to a given location divided by the surface area (cross-section of the contact region) in that location, as illustrated in figure 9.

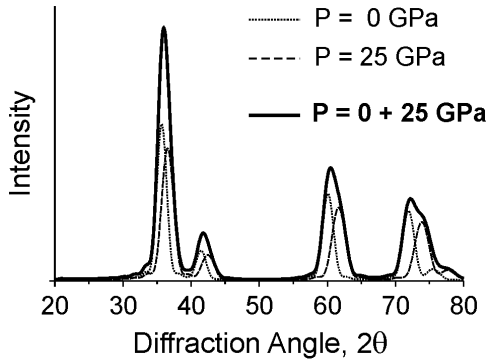

Figure 10. Diffraction patterns calculated for 10 nm SiC grains with a relaxed ($a = 4.35$ Å) and compressed ($a = 4.25$ Å at $P = 25$ GPa) lattice, dotted and dashed curves, respectively.

In the absence of a pressure medium (also in cases where the individual particles are bathed in the pressure medium but remain in direct contact) one should talk rather about distribution of stresses than about the pressure applied to the sample. In nanocrystalline materials with particles of only a few nanometres in diameter the number of contact points is very large (in the volume of 1 μm^3 the number of particles 5 nm in diameter is approximately 10^8, the number of contact points about 10^9) and distribution of stresses is quite homogenous. To simplify the description of the experiment we use the term 'pressure' as determined with the pressure marker. The marker shows a uniform distribution of stresses in the individual Au grains as confirmed by the absence of *micro*-strains in the material (no change in the width of the marker's reflections with a change in pressure indicates accumulation of the elastic energy only in *macro*-strains). Therefore we can assume that our results on strains under isostatic pressure conditions refer to essentially hydrostatic pressure conditions of the marker present in the sample.

Interpretation of an experiment performed under hydrostatic pressure is relatively simple and unambiguous. The results can be used to determine the bulk modulus or, with a more elaborate analysis, can provide the equation of state describing the lattice compression in the entire pressure range. However, an analysis of strains is never completely unambiguous: one has to account for the fact that the energy transferred to the sample through the external load is accumulated not only as the elastic energy of the crystal lattice (manifesting itself as a change of the lattice parameters and its distribution about the average value) but in other forms of energy as well (see below). Therefore, although the diffraction pattern contains complete information on *macro*- and *micro*-strains, a high pressure experiment can reveal only the factors contributing to the characteristic diffraction patterns of the crystalline phases present in the sample. Information on *macro*-strains is obtained directly from the change of positions of the Bragg reflections (change of the lattice parameters). Information on *micro*-strains is extracted, at first approximation, from the width of the Bragg reflections. *Micro*-strain is a localized state and changes from place to place in the sample volume, thus the information is the average for the entire sample. Some forms of energy have no effect on Bragg reflections and cannot be measured quantitatively, e.g. the presence of an amorphous phase is not associated with any characteristic Bragg reflections and its change under pressure cannot be detected with diffraction methods. Some sources of possible errors in the interpretation of *macro*- and *micro*-strains evaluated from powder diffraction patterns originate from inhomogenous distribution of stresses in the sample volume, as illustrated in figure 10. The figure shows

theoretical diffraction patterns calculated for 10 nm SiC grains with a relaxed cubic lattice, and a similar pattern calculated for the same lattice but compressed under hydrostatic conditions (the lattice parameter was calculated from the bulk modulus of SiC). The calculations were done using the Debye functions [55, 56]. In both cases it was assumed that all grains have the same size and contain no microstrains. The shape of the calculated Bragg reflections is purely Gaussian and the widths of the corresponding peaks are identical for both pressures (figure 10). The third pattern is the sum of these two theoretical patterns. It simulates a pattern of the sample being a mixture of equal amounts of relaxed and compressed SiC grains. (This situation may occur in samples where the external stress is not transferred to all parts of the sample volume, e.g. during high pressure densification of agglomerated powders with closed pores.) This composite pattern resembles that of a single-phase sample with the average lattice parameter corresponding to that under the pressure of 12.5 GPa. The apparent broadening of the composite peaks implies the presence of strong *micro*-strains in the sample which actually is not the case (cf section 5.2, figures 13 and 14).

5.1. Determination of macro- and micro-strains from asymmetric Bragg reflections

It is often observed that the shape of the Bragg reflections becomes asymmetric under pressure. That effect is the result of the presence of *micro*-strains in the material. The asymmetry of the reflections requires some special procedures to determine their real position and the corresponding lattice parameters. As long as relative changes of the lattice parameters are used to evaluate *macro*-strains present in the material, the specific method of evaluation of peak positions is not critical. It should, however, be applied consistently thoroughout the study and its shortcomings should be taken into account. We examined changes of the lattice parameters and peak widths with pressure using two procedures.

(1) The peak positions were measured at the weighted centre of intensity of the reflections. For symmetric reflections the centre of intensity coincides with the peak maximum; for asymmetric ones the weighted centre is shifted relative to the maximum. FWHM (full width at half maximum) was used as the peak width.
(2) The asymmetric peak shapes were approximated by a combination of two simple shape functions, Gaussian and Lorentzian, or two functions of the same type, either Lorentzian or Gaussian [36, 57] (figure 10). Assuming a complex shape of the individual intensity maxima, changes of the lattice parameters and widths (FWHMs) of the component peaks can be traced separately for each of the peak shape components (cf splitting Bragg reflections into the Gaussian and Lorentzian components for the analysis of strains in copper single crystals [58]). We used this procedure for the description of experimental data of SiC.

An example of experimentally measured asymmetry of Bragg peaks of SiC powder is shown in figure 11. Note that the peak profile measured for the standard sample was found to be 95% Gaussian [49], therefore the experimentally determined contributions from the Lorentzian shapes are due to the samples themselves. Without external pressure the positions of the peak maxima and the weighted peak centres coincide (figure 11(a)). With an increase in pressure the weighted centre of each peak shifts to the right (towards smaller d-values) relative to the peak maximum. The positions of the Gaussian and Lorentzian components of the peak move to the left- and right-hand sides of the peak maximum, respectively (figures 11(b) and (c)). We attribute this effect to non-uniform distribution of strains in the densified SiC powders (see below).

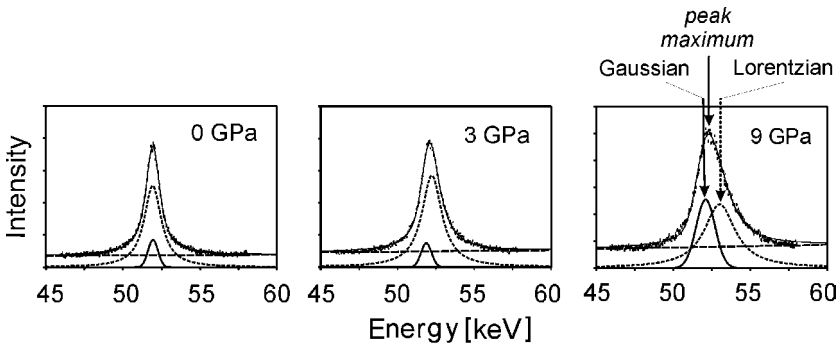

Figure 11. (111) reflections of 10 nm SiC crystals measured under different pressures.

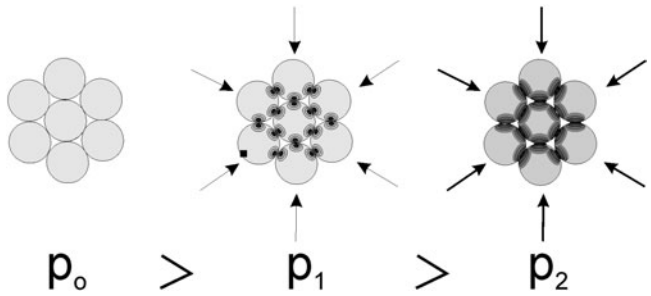

Figure 12. Tentative model of distribution of microstrains developed in individual powder particles densified under isostatic pressure conditions with an increase of external stresses.

As illustrated in figure 9, an external load applied to a porous sample propagates in the material through contact points between individual grains. At low pressures/low compression the contact areas between the grains are small and, therefore, extreme stresses and, consequently, *micro*-strains develop at the contact points (figure 12). The shape of the formed stress fields is approximately spherical [36]. With an increase in the applied external stress the contact areas increase and, simultaneously, the gradients of the stresses within the volume of the individual grains decrease. The strongly compressed parts of the grains can be regarded as domains of the same material accumulating very strong stresses and thus showing average values of the lattice parameters much smaller than that of the grain interior. Asymmetry of the Bragg reflections can be interpreted as arising from the presence of those strongly stressed domains at the contact points between the individual crystallites.

5.2. Experimental verification of models of distribution of strains in nanocrystalline SiC densified under very high isostatic pressures

Development of strains was determined from the diffraction patterns obtained under different pressures up to the maximum of 40 GPa. SiC powders used for our experiments were from three sources and were synthesized using three different methods [59–61]. We characterize these powders by the average grain size. However, the real samples have some distribution of the grain size and, therefore, the dependence of their behaviour on pressure cannot be associated with specific grain dimensions. For evaluation of the grain size distribution we used an analytical formula derived with the assumption of a log-normal grain distribution

shape using peak widths measured for a single Bragg line at one-fifth and four-fifths of its maximum [62]. The shapes of the distribution functions of the SiC samples are very similar, with the distribution becoming somewhat narrower with an increase in the grain size: for the average grain size of 2, 10 and 30 nm the dispersion σ is 1.5, 5.5 and 15, respectively. We have to emphasize that all relations between *micro*- and *macro*-strains developed under pressure should be interpreted rather as tendencies than as definite relations between the grain size and its properties.

The change of the lattice parameter with pressure determined from the weighted average positions of (111) Bragg reflections of SiC powders with 8, 10 and 30 nm average grain size is shown in figure 13(a). The same experimental data split into two peak components, Lorentzian and Gaussian (cf figure 11), are shown in figure 13(b). (*Note: according to the discussion on the meaning of the term 'lattice parameter' in section* 3.2, *we use the term alp which, in this particular case, is associated with the (111) reflection.*) In the low pressure range (up to 3–4 GPa) the lattice parameters shown in figure 13(a) decrease very rapidly with an increase in pressure. The compression of the sample resembles that of such a soft material as gold. In the pressure range from 4 to 15 GPa the apparent compression of SiC is very low (the material resembles the compression of diamond). At pressures higher than 15 GPa the compressibility assumes an intermediate value, smaller however than that corresponding to the bulk compressibility of SiC. The dependence of the lattice parameter on pressure is similar for all grain sizes except for the middle pressure range where compression is higher for powders with smaller grains. Due to isostatic pressure conditions, the observed changes of the lattice parameter may be attributed not only to the elastic properties of the crystal lattice demonstrated by *macro*-strain but also to the presence of strong *micro*-strains in the sample material which may also affect the positions of the Bragg reflections. The origin of such behaviour can be similar to that shown in figure 10: in the presence of very strong stress gradients a large portion of the sample may not contribute to the Bragg reflection (a large part of the scattered intensity is distributed over a large diffraction vector interval and gets incorporated into the backgroud intensity). That may lead to underestimation of the actual pressure acting on the sample.

Anomalous effects similar to the above of the materials' compression on pressure in the low pressure region were reported for a variety of crystalline and quasi-crystalline materials of grain size in the micron range compressed in a pressure medium [49, 63]. There is an important difference between very hard and brittle SiC and much softer and plastic materials (Cu_3Au and icosahedral Ti–Zr–Ni) in which such effects were observed. Anomalous compression behaviour in Cu_3Au was interpreted as the presence of four distinct regions where different elastic properties of Cu_3Au and of the pressure transmitting medium play a crucial role. The important feature of that phenomenon is transmission of shear stresses by the medium. The high initial compressibility occurs when the shear stresses transmitted by the pressure medium are below the yield stress of the sample. In our case no pressure transmitting medium is present but its role seems to be played by the surface of the grains. The hardening observed in Cu_3Au can be explained by repulsion between defects generated in the first pressure region during the initial strong compression. In our samples we attribute this effect to generation of defects at the surface of the grains. Similar behaviour observed in icosahedral Ti–Zr–Ni was explained by its low shear modulus and high Poisson ratio, and by very strong pressure gradient with uniaxial stress component in the DAC. Very high compressibility at low pressure followed by hardening can be interpreted as a property closely related to elastic and plastic properties of alloys. Similar behaviour occurring in nanocrystalline SiC constitutes an 'overall property' of the materials that is clearly related to the grain size but is due to the specific properties of the surface which transmits the stress. The ratio of the numbers of surface to bulk atoms determines the behaviour of the material under pressure.

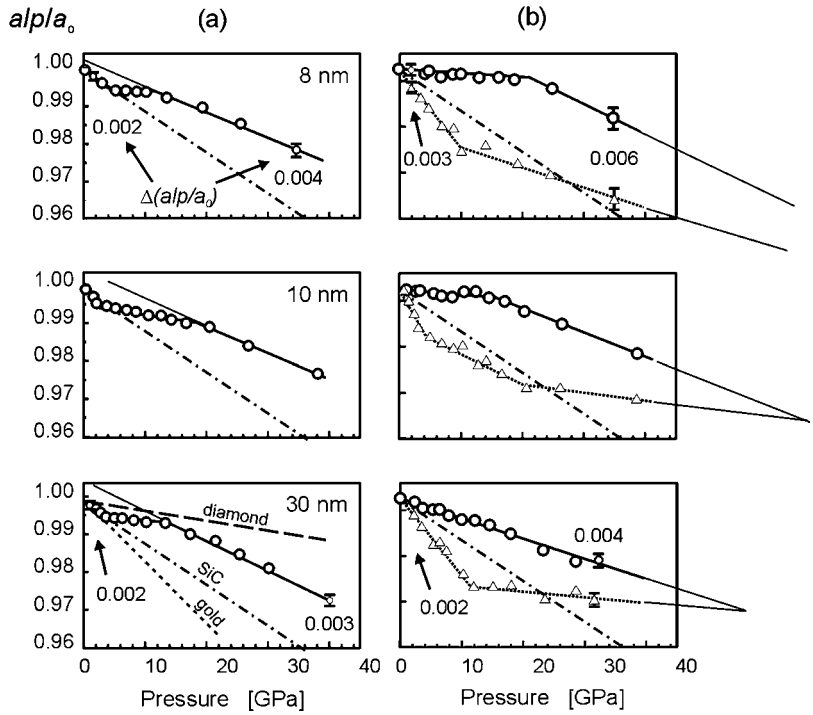

Figure 13. Relative lattice parameter of SiC nanocrystals as a function of isostatic pressure for different grain sizes. (a) Solid lines and open circles—lattice parameters as determined from the weighted average positions of the (111) Bragg reflections; (b) lattice parameters as determined from the positions of the Gaussian (dashed lines and open triangles) and Lorentzian (dotted lines and solid triangles) components of the peak shape functions. Dash–dotted lines—regular compression curves of bulk SiC.

Figure 13(b) shows an alternate method of data elaboration which is based on separation of Gaussian and Lorentzian components of the Bragg reflections. As can be seen in the figure the two components behave very differently under pressure. Up to three pressure ranges can be distinguished. At lower pressures the compression described by the Gaussian component is always much smaller than that corresponding to the Lorentzian one (figure 13(b)). Apparently the Lorentzian component reflects the presence of extreme stresses which develop at inter-grain contact points. Those local stresses become smaller with an increase in the external stress which is an apparent result of an increase of the contact area between the grains as the densification proceeds. The stresses at the contact surface are always much higher than those in the interior of the grains which, as a result, remains compressed less than the surface. We presume that the compression of the interior of the grains is described by the Gaussian peak component. A strong compression at the surface (where most of the elastic energy of the SiC lattice is accumulated) makes the grain surface much harder than the interior of the grains. In the compact the surfaces of individual grains merge into inter-grain boundaries which are actually denser, and thus harder than the rest of the material (the interior of the grains). We suggest that this happens because the dense boundaries form a kind of a very hard matrix (skeleton), like that shown in figure 12, and protect the grain interior from the external stress (figure 13(b)). Following this concept of the mechanism of densification, the effect of surface hardening should diminish with an increase in the grain size since the protective effect of the hardened surface layer (which is a part of the interface) is much less effective for larger grains

where smaller fractions of atoms form the boundaries. This is consistent with the fact that the largest difference between the Gaussian and Lorentzian plots in figure 13(b) is observed for the smallest grains, and that the difference between the lattice parameters measured for both peak components decreases with an increase in pressure faster for larger than for smaller grains. As the density of the sample increases, the total area of contacts between the grains increases and the amount of *micro*-strain levels off. At sufficiently high pressures the material should approach the theoretical density and the lattice parameters determined from the Bragg lines should correspond to those calculated directly from the compressibility of the material. A fully dense, homogenous material would produce symmetric Bragg peaks and, thus, at sufficiently high pressures the positions of Lorentzian and Gaussian components shown in figure 13(b) should merge; that may be expected to happen at about 50 GPa for 30 nm, 60 GPa for 10 nm, and at higher pressures for 8 nm SiC powder.

Another important aspect of analysis of hp diffraction data is the question of how much of the external energy of the sample under stress (the external stress) is accumulated in the sample in the form of the elastic energy of the crystal lattice. Assuming that there is a similar 'efficiency' of transfer of external energy into different SiC samples, no effect of the grain size on the overall compression of the material should exist, i.e. no change of the average value of the lattice parameter measured from the Bragg reflections should be observed. The compression plots in figure 13(a) obtained from weighted average positions of the Bragg reflections (i.e. positions corresponding to the average lattice parameters) show similar behaviour. There are, however, some differences which indicate that not all of the external energy is transferred into the elastic energy of the SiC lattice. We discuss this point below based on the analysis of *micro*-strains evaluated from peak widths measured for SiC powders with grains from 2 to 30 nm exposed to pressures of up to 40 GPa.

The relative change of the lattice parameters (the measure of *macro*-strains) and FWHM (the measure of *micro*-strains) with pressure for SiC powders with different grain sizes is shown in figures 14(a) and (b), respectively. (In this study we did not attempt to separate (split) the measured peaks into two components because of a very large broadening of the peaks making such analysis ambiguous.) Figure 14 shows the effect of pressure on *macro*- and *micro*-strains generated in SiC which are obviously dependent on the average size of the grains. At the initial stage of densification, up to several gigapascals, a very strong decrease of the as-measured lattice parameters is observed for all samples, consistent with figure 13. With further increase in the external stress, for a certain pressure interval nearly constant values of the lattice parameters are observed (for all samples). This pressure interval ends at lower pressures for larger grain size powders. (*Note that the smallest grain powder shows a specific behaviour: two subsequent steps of a strong decrease followed by a pressure interval of a constant lattice parameter. This is probably related to a special microstructure of SiC, a subject that is not discussed further in this paper.*) Above a certain pressure, different for different materials and marked by the arrows, the compression of the nanopowders shows normal behaviour and is very similar to that corresponding to the bulk modulus of SiC. In the initial, non-linear parts of the compression curves (figure 13(a)) the changes of the lattice parameter are much smaller than might be expected from simple lattice compression of SiC corresponding to the applied external pressure. This is obviously related to generation of *micro*-strains reflected in broadening of the Bragg reflections (figure 13(b)). Generation of microstrains leads to a pressure offset: the materials reach elastic compressibility of the SiC lattice at higher pressures. In the pressure range where micro-strains are generated the width of the Bragg peaks shows no or a very limited increase with an increase in pressure. (From this point on the compression of the samples represented by the change of the lattice parameters agrees well with the compressibility of bulk SiC.)

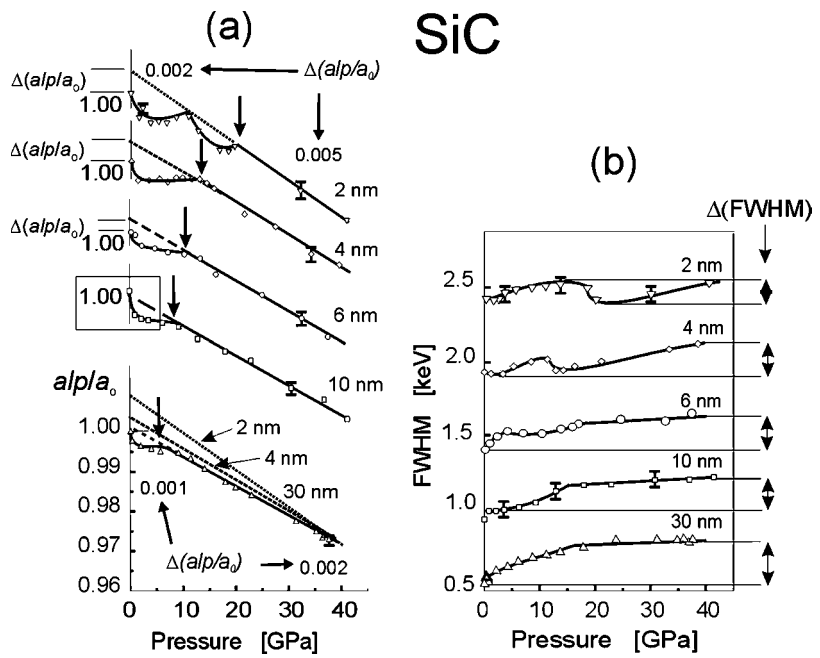

Figure 14. Effect of pressure on the structure of SiC nanocrystals for different size grains. (a) Relative change of the interplanar spacings (the arrows mark the upper limit of major deviations from the regular compression curves); (b) change of FWHM of the Bragg reflections.

The character of change of broadening of the Bragg reflections with pressure in SiC (i.e. the development of *micro*-strains and their distribution) clearly depends on the grain size. The total increase in the width of the Bragg reflections over the pressure range of 0–40 GPa decreases with the grain size (figure 14(b)). That phenomenon can be explained by the fact that in a powder with smaller grains the total number of contacts between individual grains is larger and, therefore, the gradients of local stresses (and, thus, *micro*-strains) are smaller. Accordingly, an increase in the width of the Bragg reflections with an increase in pressure is smaller. However, the portion of the total energy accumulated in the material which has no effect on the overall compression of the material as measured from the Bragg lines is larger for smaller grain size powders. This is reflected by a kind of a 'shift of the elastic compression range' exhibited as the difference between the lattice parameter of the SiC lattice under normal pressure and the value extrapolated to normal pressure from the compressibility plot at high pressures; this difference is shown in figure 14(a) as $\Delta(\mathrm{alp}/a_0)$. The value of $\Delta(\mathrm{alp}/a_0)$ is obviously proportional to the relative number of the atoms located at the interfaces. That suggests that only a part of the external energy is accumulated in the elastic energy of the SiC lattice. Further discussion of this problem is outside the scope of this work.

5.3. Application of the core–shell model to interpretation of hp diffraction experiments on SiC nanocrystals

So far we have attempted to interpret the change of the diffraction patterns of nanocrystals measured under high pressures in terms of generation of strains in a well defined, uniform crystallographic phase material. An alternate interpretation of the diffraction data of nanocrystals can be based on a two-phase model of a nanocrystalline grain. Such a model

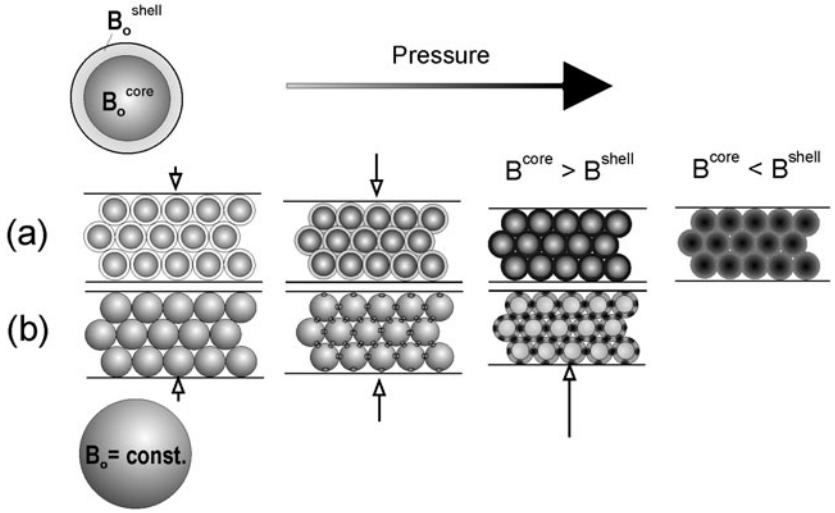

Figure 15. Distribution of strains under isostatic pressure. (a) Two-phase (core–shell) powder grains; (b) grains with a uniform initial structure.

assumes that the atomic structures and properties of the grain core and of the surface differ from each other [6–8]. Consequently, the elastic properties of the grain cores and surfaces are different too and the behaviour of such nanocrystals under pressure can be interpreted as being the result of the presence of two phases with different elastic properties. Below we present a tentative interpretation of our diffraction data based on such a model.

In a simple core–shell model the grain core is surrounded by a surface shell with its structure similar to that of the core but compressed or expanded relative to the relaxed lattice (cf section 3.2). It is obvious that the elastic properties (bulk modulus B_0) of the surface shell (B_0^{shell}) are different from the compressibility of the crystal lattice of the grain core (B_0^{core}). The mechanism of compression of a powder of spherical grains with two- and one-phase structures is illustrated in figures 15(a) and (b), respectively. The surface shell (model a) can be either harder or softer than the grain core. Under external stress the compression of the surface shell is respectively smaller or larger than that of the core. The compression proceeds approximately linearly with an increase in pressure in the elastic region and the lattice hardens (its bulk modulus increases) at sufficiently high pressures. When the surface shell is softer than the core, the surface compresses under external stress more than the core. The grain surfaces merged into grain boundaries constitute a kind of a matrix embedding the grain cores (cf figure 12). This matrix of the grain boundaries hardens under stress and accommodates most of the applied external stresses and, thus, the stress transferred to the grain cores becomes significantly reduced. As a result, the cores are 'undercompressed', i.e. less compressed than might be expected from the average pressure in the sample volume (figure 15(a), the model with $B_0^{\text{core}} > B_0^{\text{shell}}$). The matrix of the grain boundaries may be expected to have some strength limitations above which it would break up and allow for a more direct transfer of the external stress to the grain cores. At sufficiently high pressures the bulk moduli of the core and surface components may be expected to become equal and the sample to assume the character of a uniform phase material.

The above postulated mechanism of hardening of the surface shells of the grains, and the resulting formation of hard boundaries between the grains, is qualitatively consistent with

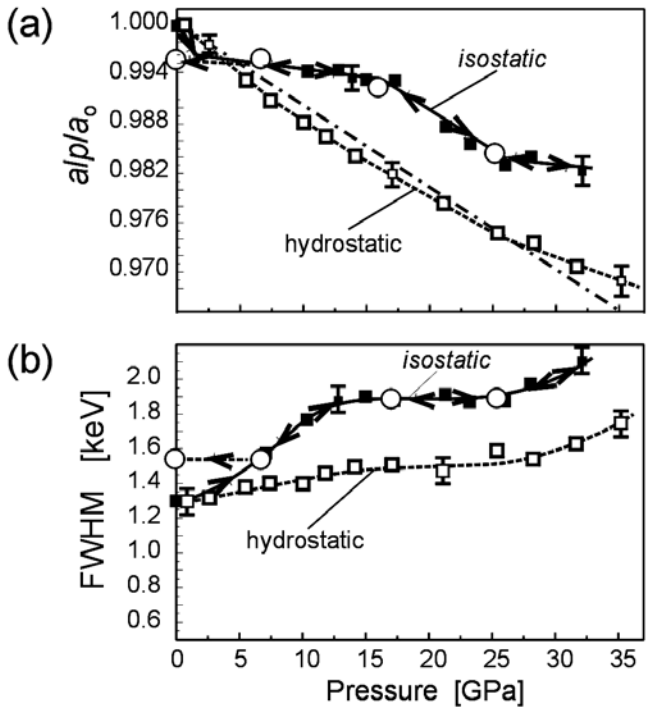

Figure 16. Effect of pressure on strains in 8 nm SiC crystals. Solid squares and solid curves—isostatic, open squares and dotted curves—hydrostatic conditions, circles—points obtained during the samples' decompression. (a), (b) Relative changes of the lattice parameters and the reflection widths (FWHMs), respectively; dash–dotted curve—regular compression curve of SiC.

the model of a very strong local strain field generated at the contact points between the grains which we applied for the analysis of the diffraction experiments showing a strong asymmetry of the Bragg reflections (figures 13 and 14). Under isostatic pressure conditions the distributions of strains in powders with one phase and a core–shell type structure of the individual grains should be very similar: under pressure the strains at the surface would exceed that in the grain interior in both cases. That implies that investigation of compression under isostatic pressure conditions may hardly allow us to distinguish between one- and two-phase nanocrystalline grains. The actual type of the initial structure can be identified by performing and comparing the results of related experiments conducted under isostatic and hydrostatic pressure conditions.

5.3.1. Hydrostatic versus isostatic pressure conditions. Under hydrostatic pressure conditions the compression curves of one-phase grains may be expected to yield a change of the lattice parameters corresponding to the lattice compressibility of the material. Figure 16(a) shows compression of nanocrystalline SiC under hydrostatic and isostatic pressures. There is a clear difference between the two compression curves at low pressures, and obvious similarities above 15–20 GPa. A similar character of the curves (attributed to formation of *micro*-strains) is observed in figure 16(b): a very strong increase of reflection broadening in isostatically compressed powder up to the pressure of 10–15 GPa, followed by a parallel run of the curves above 15 GPa where similar *micro*-strains are generated under iso- and hydrostatic conditions.

The above analysis leads us to the conclusion that not the one- but the two-phase model of nanocrystals is appropriate for the description of the behaviour of nanocrystalline SiC under

pressure. Additional support for this model comes with the application of our concept of the 'apparent lattice parameter', alp (cf section 3.2).

5.4. Application of the alp concept to interpretation of the hp diffraction experiment

As we have shown in several papers, the presence of the surface shell compressed or expanded relative to the grain core leads to a strong change of the alp parameters, calculated for individual Bragg reflections at small Q-values, relative to the relaxed lattice [6–8]. For powder diffraction performed *in situ* under high pressure using x-ray radiation the experimentally accessible Q-range is limited to small Q-values (<5 Å^{-1}). Such a Q-range is too narrow for an accurate determination of the specific values of interatomic distances describing the model, but is sufficient for an evaluation of the effect of compression of the surface layer on the measured alp values. Figure 17 shows the experimental alp values determined for three Bragg reflections measured under both isostatic and hydrostatic compression conditions plotted versus the diffraction vector Q for different pressures. The change of alp is non-linear with pressure, depends on the Q-value (i.e. on the Bragg reflection), and is different for isostatic and hydrostatic conditions. Based on our numerical simulations of the alp–Q-plots for nanograins with a core–shell structure we were able to identify and evaluate the strain present in the surface shell of the grains. We calculated the theoretical alp–Q-plot corresponding to that measured experimentally at normal pressure (relaxed structure) for the model of a 10 nm SiC nanocrystal shown in figure 17(c). Figure 17(d) shows the model corresponding both to the alp–Q-plot obtained at 1.5 GPa under isostatic conditions and that obtained at 5 GPa under hydrostatic pressure.

The analysis of the alp–Q-plots presented above provides a (tentative) interpretation of the results of our hp diffraction experiments discussed in previous sections. As seen in figure 17, the reflections observed at small Q-values are very sensitive to the structure of the surface of the grain and, therefore, the analysis of singular Bragg reflections is insufficient for evaluation of the real lattice parameters. With an increase in the applied hydrostatic pressure a changing compression leads to a change of the initial relation between the interatomic distances in the core and the shell. The tensile strain in the surface shell observed in the starting material converts to a compressive strain under the external stress (figure 17(a)) (the tensile or compressive type of strain is determined by comparing the actual lattice parameter with that in the grain core). A similar behaviour of identical SiC samples exhibited both under hydrostatic (figure 17(b)) and isostatic (figure 17(a)) conditions provides a clear indication that the origin of changes of alp values with Q has common roots. The change of the shape of the alp–Q-plot for isostatic compression is much stronger than that under corresponding hydrostatic pressure conditions. That is understandable because stronger stress gradients between core and surface develop when individual grains are in direct contact. From that we conclude that the observed difference between alp–Q-plots obtained under hydrostatic and isostatic pressures results from a difference in the elastic properties of the grain surface and its core; the surface shell with the initial tensile strain has apparently a larger compressibility (smaller bulk modulus) than the grain core.

6. Summary

In this work we performed an analysis of the diffraction data collected on nanocrystalline SiC samples applying several methods of elaboration. We were looking for differences between the behaviour of powders of the same material but of different grain sizes. We examined *micro*- and *macro*-strains and tried to determine the overall bulk modulus which might be

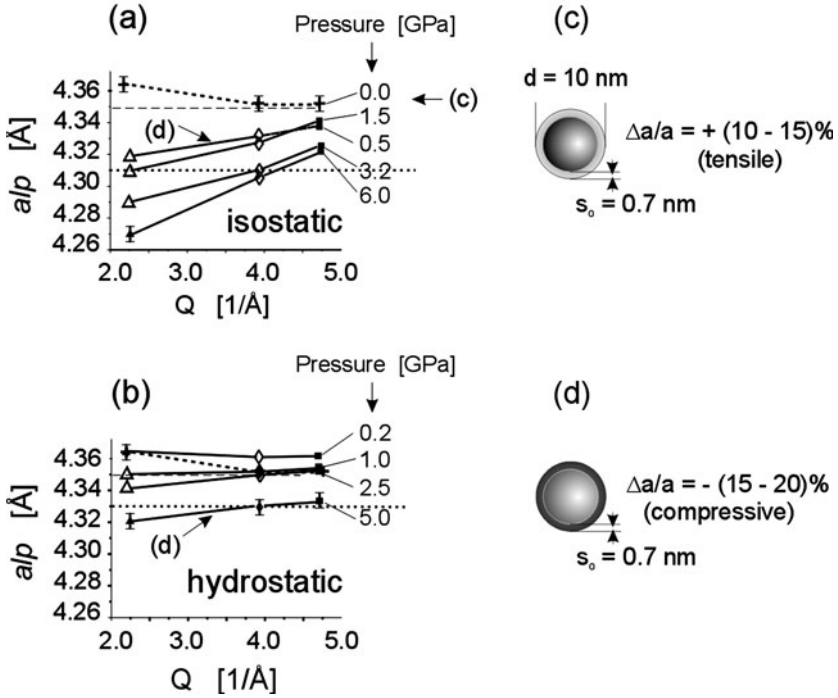

Figure 17. Alp–Q-plots of 10 nm grain nanocrystalline SiC powder measured under pressure. (a) Isostatic pressure; (b) hydrostatic pressure; (c) a model of a 10 nm SiC grain of the starting material with tensile strain; (d) a model of the SiC grain with the compression strain in the surface layer. Dashed line, lattice parameter of the core of the model; dotted line, the lattice parameter under the pressure of 5 GPa calculated from the bulk compressibility of SiC, $\Delta\text{alp} = \pm 0.005$ Å.

a size dependent property of the material. Indeed, such dependence might occur due to the presence of internal pressure in as-synthesized nanograins, as suggested earlier in the literature [64–68]. We showed that densification of nanocrystals always proceeds through several stages and that it is practically impossible to derive a unique value of the overall bulk modulus (quantifying compression of the lattice parameters) from the positions of the Bragg reflections. Densification of powders without a pressure medium and during compression under pseudo-hydrostatic conditions (with silicon oil as a pressure medium) show similar behaviour of the samples. Under both conditions strong *micro*-strains are generated, and they significantly affect the actual positions of the Bragg reflections which become inconsistent with the compressibility of the crystal lattice of a given material. We suggest that the origin of *micro*-strains is twofold: (i) different elastic properties of the grain cores and shells, and (ii) the presence of very strong stresses at the contact points between individual grains.

In our opinion, the issue of a unique compressibility of nanocrystals and its dependence on the grain size is practically impossible to solve. The situation is similar to that which we faced when looking for the 'lattice parameters' of very small crystals and expected to get a unique answer from a diffraction experiment. As we showed in our earlier papers [6–8], examination of the experimental diffraction data using tools originally developed for large crystals with dimensions several orders of magnitude larger than the unit cell is inadequate for nanocrystals. Consequently, we suggested an application of the so-called 'alp' value which can be derived experimentally and used instead of the 'lattice parameter' for characterization of very small

crystals. In this work we showed that a similar method of data elaboration, i.e. determination of the alp values for different diffraction vectors Q, can be applied for a description of changes of diffraction patterns of nanocrystals exposed to external stresses.

Recently we showed that PDF analysis of diffraction data gives clear evidence that interatomic distances in nanocrystalline diamond and SiC change with size when the grain diameter is smaller than 20 nm [8, 69]. Similar PDF analysis of changes of interatomic distances in nanocrystals measured *in situ* would be very important for a description of high pressure diffraction experiments.

Acknowledgments

This work was supported by the Polish Committee for Scientific Research grant PBZ/KBN-013/T08/30, the Polish–German project POL-00/009, and in part by the EC grant 'Support for centres of excellence' No ICA1-CT-2000-70005, DESY-Hasylab Project II-99-053. S Stel'makh gratefuly acknowledges support from the Roman Herzog Program of the Alexander von Humboldt Foundation. The work was also supported by the Office of Biological and Physical Sciences of NASA.

References

[1] Navrotsky A 2001 Thermochemistry of nanomaterials *Nanoparticles and the Environment* (*Reviews in Mineralogy and Geochemistry* vol 44) ed J F Banfield and A Navrotsky (Washington, DC: Mineralogical Society of America)
[2] Jacobs K and Alivisatos A P 2001 Nanocrystals as model systems for pressure-induced structural phase transitions *Nanoparticles and the Environment* (*Reviews in Mineralogy and Geochemistry* vol 44) ed J F Banfield and A Navrotsky (Washington, DC: Mineralogical Society of America)
[3] Couchman P R and Jesser W A 1977 *Nature* **269** 481
[4] Hirth J P and Lothe J 1982 *Theory of Dislocations* (New York: Wiley)
[5] Gleiter H 2000 *Acta Mater.* **48** 1
[6] Palosz B, Grzanka E, Gierlotka S, Stel'makh S, Pielaszek R, Lojkowski W, Bismayer U, Neuefeind J, Weber H-P and Palosz W 2002 *Phase Transit.* **76** 171
[7] Palosz B, Grzanka E, Gierlotka S, Stel'makh S, Pielaszek R, Bismayer U, Neuefeind J, Weber H-P and Palosz W 2002 *Acta Phys. Pol.* A **102** 57
[8] Palosz B, Grzanka E, Gierlotka S, Stel'makh S, Pielaszek R, Bismayer U, Neuefeind J, Weber H-P, Proffen Th, Von Dreele R and Palosz W 2002 *Z. Kristallogr.* **217** 497
[9] Bish D L and Post J E 1989 *Modern Powder Diffraction* (*Reviews in Mineralogy* vol 20) (Washington, DC: Mineralogical Society of America)
[10] Young R A 1993 *The Rietveld Method* (Oxford: International Union of Crystallography–Oxford University Press)
[11] Klug H P and Alexander L E 1954 *X-Ray Diffraction Procedures* (New York: Wiley)
[12] Billinge S J L and Thorpe M F 1998 *Local Structure from Diffraction* (New York: Plenum)
[13] Loeffler L and Weissmueller J 1995 *Phys. Rev.* B **52** 7076
[14] Zhu X, Birringer R, Herr U and Gleiter H 1987 *Phys. Rev.* B **35** 9085
[15] Lue J T 2001 *J. Phys. Chem. Solids* **62** 1599
[16] Choi C J, Dong X L and Kim B K 2001 *Scr. Mater.* **44** 2225
[17] Harada J and Ohshima K 1981 *Surf. Sci.* **106** 51
[18] Solliard C and Flueli M 1985 *Surf. Sci.* **156** 487
[19] Woltersdorf J, Nepijko A S and Pippel E 1981 *Surf. Sci.* **106** 64
[20] Montano P A, Shenoy G K, Alp E E, Schulze W and Urban J 1986 *Phys. Rev. Lett.* **56** 2076
[21] Tolbert S H and Alivisatos A P 1995 *J. Chem. Phys.* **102** 4642
[22] Lan Y C, Chen X L, Xu Y P, Cao Y G and Huang F 2000 *Mater. Res. Bull.* **35** 2325
[23] Boswell F W C 1951 *Proc. Phys. Soc.* A **64** 465
[24] Beck Ch, Ehses K H, Hempelmann R and Bruch Ch 2001 *Scr. Mater.* **44** 2127
[25] Zhao Y H, Zhang K and Lu K 1997 *Phys. Rev.* B **56** 14322

[26] Brown R C 1947 *Proc. R. Soc.* **59** 429
[27] Defay R and Prigogine I 1966 *Surface Tension and Adsorption* (London: Longmans)
[28] Cammarata R C 1992 *Surf. Sci. Lett.* **273** L399
[29] Cammarata R C 1997 *Mater. Sci. Eng.* A **237** 180
[30] Gilman J J 1960 *J. Appl. Phys.* **31** 2208
[31] Mays C W, Vermaak J S and Kuhlmann-Wilsdorf D 1968 *Surf. Sci.* **12** 134
[32] Shuttleworth R 1950 *Proc. Phys. Soc.* A **63** 444
[33] Stoneham A M 1977 *J. Phys. C: Solid State Phys.* **10** 1175
[34] Vermaak J S, Mays C W and Kuhlmann-Wilsdorf D 1968 *Surf. Sci.* **12** 128
[35] Borel J-P and Chatelain A 1985 *Surf. Sci.* **156** 572
[36] Eremets M 1996 *High Pressure Experimental Methods* (Oxford: Oxford University Press)
[37] Buras B and Gerward L 1989 *Prog. Cryst. Growth Charact.* **18** 93
[38] Defay R and Prigogine I 1966 *Surface Tension and Adsorption* (London: Longmans)
[39] Wolf D and Merkle K L 1992 *Materials Interfaces: Atomic Level Structure and Properties* ed D Wolf and S Yip (London: Chapman and Hall) p 87
[40] Howe M J (ed) 1997 *Interfaces in Materials* (New York: Wiley)
[41] Wolf D and Yip S (ed) 1992 *Materials Interfaces; Atomic Level Structure and Properties* (London: Chapman and Hall)
[42] Palosz B, Grzanka E, Gierlotka S, Stel'makh S, Pielaszek R, Bismayer U, Neuefeind J, Weber H-P and Palosz W 2002 *Mechanics of Advanced Materials* (*Lecture Notes* vol 4) ed Z Mróz (Warsaw: Center of Excellence for Advanced Materials and Structures) pp 235–306
[43] Pielaszek R, Aloshina M, Palosz B, Gierlotka S and Stel'makh S 1998 *Mater. Res. Soc. Symp. Proc.* **501** 305
[44] Palosz B, Stel'makh S, Gierlotka S, Aloshina M, Pielaszek R, Zinn P, Peun Th, Bismayer U and Keil D G 1998 *Mater. Sci. Forum* **278–281** 612
[45] Palosz B, Gierlotka S, Stel'makh S, Pielaszek R, Zinn P and Bismayer U 1999 *Mater. Sci. Forum* **286** 184
[46] Pielaszek R, Palosz B, Gierlotka S, Stelmakh S and Bismayer U 1999 *Mater. Res. Soc. Symp. Proc.* **538** 561
[47] Grzanka E, Palosz B, Gierlotka S, Pielaszek R, Bismayer U, Janik J F, Wells J R, Palosz W and Porsch F 2002 *Acta Phys. Pol.* A **102** 167
[48] Otto J W, Vasiliou J K and Frommeyer G 1997 *J. Synchrotron Radiat.* **4** 155
[49] Otto J W 1997 *Nucl. Instrum. Methods Phys. Res.* A **384** 552
[50] Neuling H W and Holzapfel W B 1992 *High Pressure Res.* **8** 655
[51] Weidner D J, Vaughan M T, Ko J, Wang J, Liu X, Yeganeh-Haeri A, Pacalo R E and Zhao Y 1992 Characterization of stress, pressure, and temperature in SAM85, a DIA type high pressure apparatus *High-Pressure Research: Application to Earth and Planetary Sciences* ed Y Syono and M H Manghnani (Tokyo: Terra) pp 13–7
[52] Weidner D J, Wang Y and Vaughan M T 1994 *Geophys. Res. Lett.* **21** 753
[53] Zhao Y, Weidner D J, Ko J, Leinenweber K, Liu X, Li B, Meng Y, Pacalo R E G, Vaughan M T, Wang Y and Yeganeh-Haeri A 1994 *J. Geophys. Res.* B **99** 2871
[54] Bish D L and Post J E 1989 *Modern Powder Diffraction* (*Reviews in Mineralogy* vol 20) (Washington, DC: Mineralogical Society of America)
[55] Bondars B, Gierlotka S and Palosz B 1993 *Mater. Sci. Forum* **133–136** 301
[56] Pielaszek R, Gierlotka S, Stel'makh S, Grzanka E and Palosz B 2002 *Defect Diffusion Forum* **208/209** 267
[57] Palosz B, Gierlotka S, Stel'makh S, Pielaszek R, Zinn P, Winzenick M, Bismayer U and Boysen H 1999 *J. Alloys Compounds* **286** 184
[58] Ungar T, Mughrabi H, Roennpagel D and Wilkens M 1984 *Acta Metall.* **32** 333
[59] Keil D G, Calcote H F and Gill R J 1996 *Mater. Res. Soc. Symp. Proc.* **410** 167
[60] Buschmann V, Klein S, Fuess H and Hahn H 1998 *J. Cryst. Growth* **193** 335
[61] Martin H-P, Müller E, Richter R, Roever G and Brendler E 1997 *J. Mater. Sci.* **32** 381
[62] Pielaszek R 2002 Diffraction studies of microstructure of nanocrystals densified under high pressures *PhD Thesis* Institute of Physics, Warsaw University (in Polish)
[63] Ponkratz U, Nicula R, Jianu A and Burkel E 2000 *J. Phys.: Condens. Matter* **12** 8071
[64] Qadri S B, Yang J, Ratna B R, Skelton E F and Hu J Z 1996 *Appl. Phys. Lett.* **69** 2205
[65] Silvestri M R and Schroeder J 1995 *J. Phys.: Condens. Matter* **7** 8519
[66] Tolbert S H and Alivisatos A P 1993 *J. Phys. D: Appl. Phys.* **26** 56
[67] Tolbert S H and Alivisatos A P 1995 *J. Chem. Phys.* **102** 4642
[68] Wickham J N, Herhold A B and Alivisatos A P 2000 *Phys. Rev. Lett.* **84** 923
[69] Palosz B, Grzanka E, Stel'makh S, Gierlotka S, Pielaszek R, Bismayer U, Weber H-P, Proffen Th and Palosz W 2003 *Solid State Phenomena* vol 94, ed W Lojkowski and J R Blizzard (Scitec) p 203